Effect of phosphate availability on biofilm formation in cooling towers

Pinel, Ingrid S.M.; Kim, Lan Hee; Proença Borges, Vitor R.; Farhat, Nadia M.; Witkamp, Geert Jan; van Loosdrecht, Mark C.M.; Vrouwenvelder, Johannes S.

DOI
10.1080/08927014.2020.1815011

Publication date
2020

Document Version
Final published version

Published in
Biofouling

Citation (APA)
Pinel, I. S. M., Kim, L. H., Proença Borges, V. R., Farhat, N. M., Witkamp, G. J., van Loosdrecht, M. C. M., & Vrouwenvelder, J. S. (2020). Effect of phosphate availability on biofilm formation in cooling towers. *Biofouling*, *36*(7), 800-815. https://doi.org/10.1080/08927014.2020.1815011

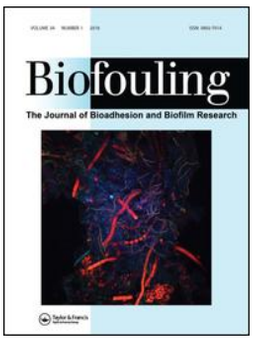

Taylor & Francis
Taylor & Francis Group

Biofouling
The Journal of Bioadhesion and Biofilm Research

ISSN: (Print) (Online) Journal homepage: https://www.tandfonline.com/loi/gbif20

Effect of phosphate availability on biofilm formation in cooling towers

Ingrid S. M. Pinel , Lan Hee Kim , Vitor R. Proença Borges , Nadia M. Farhat , Geert-Jan Witkamp , Mark C. M. van Loosdrecht & Johannes S. Vrouwenvelder

To cite this article: Ingrid S. M. Pinel , Lan Hee Kim , Vitor R. Proença Borges , Nadia M. Farhat , Geert-Jan Witkamp , Mark C. M. van Loosdrecht & Johannes S. Vrouwenvelder (2020): Effect of phosphate availability on biofilm formation in cooling towers, Biofouling, DOI: 10.1080/08927014.2020.1815011

To link to this article: https://doi.org/10.1080/08927014.2020.1815011

BIOFOULING
https://doi.org/10.1080/08927014.2020.1815011

Effect of phosphate availability on biofilm formation in cooling towers

Ingrid S. M. Pinel[a], Lan Hee Kim[b], Vitor R. Proença Borges[b], Nadia M. Farhat[b], Geert-Jan Witkamp[b], Mark C. M. van Loosdrecht[a] and Johannes S. Vrouwenvelder[a,b]

[a]Department of Biotechnology, Faculty of Applied Sciences, Delft University of Technology, Delft, The Netherlands; [b]Division of Biological and Environmental Science and Engineering (BESE), Water Desalination and Reuse Center (WDRC), King Abdullah University of Science and Technology (KAUST), Thuwal, Saudi Arabia

ABSTRACT

Phosphate limitation has been suggested as a preventive method against biofilms. P-limited feed water was studied as a preventive strategy against biofouling in cooling towers (CTs). Three pilot-scale open recirculating CTs were operated in parallel for five weeks. RO permeate was fed to the CTs (1) without supplementation (reference), (2) with supplementation by biodegradable carbon (P-limited) and (3) with supplementation of all nutrients (non-P-limited). The P-limited water contained $\leq$10 µg PO_4 l^{-1}. Investigating the CT-basins and coupons showed that P-limited water (1) did not prevent biofilm formation and (2) resulted in a higher volume of organic matter per unit of active biomass compared with the other CTs. Exposure to external conditions and cycle of concentration were likely factors that allowed a P concentration sufficient to cause extensive biofouling despite being the limiting compound. In conclusion, phosphate limitation in cooling water is not a suitable strategy for CT biofouling control.

GRAPHICAL ABSTRACT

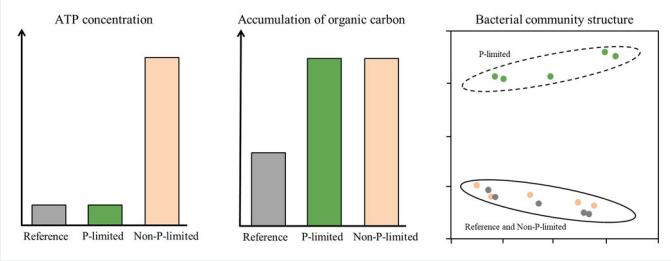

ARTICLE HISTORY
Received 5 May 2020
Accepted 20 August 2020

KEYWORDS
Biofouling; nutrient limitations; water quality; biofilm composition; microbial community analyses; principal component analysis

Introduction

Tackling biofouling is a major challenge in the operation of open recirculating cooling towers (CTs). Biofilms forming on the inner surfaces of heat exchangers, pipes and basin increase heat transfer resistance and provide a protective environment for microbial communities particularly involved in microbiologically induced corrosion (MIC) of metal surfaces or disease outbreaks (Türetgen and Cotuk 2007; Rao et al. 2009). The generated loss in cooling efficiency, occasional pipe clogging and material deterioration lead to early replacement of process parts, intense cleanings and increased chemical dosages, therefore resulting in high capital and operating costs for the industry (Melo et al. 2010).

The standard biofouling control methods consist of dosage of biocides such as sodium hypochlorite, chlorine dioxide or bromine in the cooling systems (Al-Bloushi et al. 2018; Pinel et al. 2020). Although, these chemicals considerably slow down the build-up of biofilms by deactivating planktonic bacterial cells, they cannot completely prevent biofilm formation and have little curative action. Studies have shown that biocide efficiencies strongly depend on transport limitations arising from reaction-diffusion phenomena within a biofilm (De Beer et al. 1994; Chen and Stewart 1996; Xu et al. 2000). Extracellular polymeric substances (EPS) are essential compounds that form the biofilm matrix and react with these chemicals, limiting the deactivation of the embedded active cells

CONTACT Ingrid S. M. Pinel I.S.M.Pinel@tudelft.nl
Supplemental data for this article can be accessed at https://doi.org/10.1080/08927014.2020.1815011.

(Xue et al. 2013). In addition, a high concentration of oxidative biocides is known to induce corrosion of metal surfaces such as plumbing parts and heat exchangers (Edwards and Dudi 2004).

Previous studies have suggested that the removal of essential nutrients can constitute a preventive measure against biofilm formation in industrial processes such as membrane filtration systems (Vrouwenvelder et al. 2010) and CTs (Meesters et al. 2003). As organic carbon is generally the limiting compound for microbial growth in freshwater, removal of assimilable organic carbon (AOC) is often applied to inhibit the build-up of biofilm (Daamen et al. 2000; Visvanathan et al. 2003). Different AOC thresholds have been proposed to prevent issues linked to bacterial regrowth in unchlorinated systems: $50\,\mu g\,l^{-1}$, similar to the groundwater concentration (Bradford et al. 1994), $10\,\mu g\ l^{-1}$ in drinking water systems (van der Kooij et al. 1989) or even $1\,\mu g\ l^{-1}$ against biofouling of spiral wound membranes (Hijnen et al. 2009). Reducing the AOC to such low levels is very challenging with conventional techniques such as biological filtration or activated carbon adsorption (van der Kooij et al. 1989; Nguyen et al. 2012). Importantly, microbial growth also depends on the availability of phosphorus in water (Miettinen et al. 1997; Lehtola et al. 2002). Phosphate (P)-limitation has been shown to control biofouling in reverse osmosis (RO) membrane systems in the presence of high organic concentration (Vrouwenvelder et al. 2010; Kim et al. 2014) suggesting P-removal as a suitable pre-treatment for industrial water processes. No literature is, however, available on the effectiveness of P-limitation in controlling biofouling in cooling water systems. A few studies have investigated the microbiome of biofilms from CTs (Balamurugan et al. 2011; Wang et al. 2013; Di Gregorio et al. 2017; Tsao et al. 2019), mainly focusing on MIC and the impact of disinfection, but the effect of nutrient limitations and sample location remains unexplored. In general, further investigation on the effect of nutrient limitations in cooling water would be highly valuable to the industrial field as it guides the selection of feed water, pre-treatment and chemical dosage strategies.

The choice of the feed water used in CTs depends mostly on the water sources available at the geographic locations. In Europe, most CTs are operated with freshwater (e.g. ground or surface water), causing less damage to the process than seawater, which is frequently used, for example, in the Middle-East (Al-Bloushi et al. 2018). In this study, seawater reverse osmosis (SWRO) permeate was selected as a reference feed water for three parallel pilot-scale CTs due to its ultra-low content of the elements and nutrients required for microbial growth: RO permeate water has one of the highest water qualities achievable. The pilot set-up used in this study was located on an industrial site and allowed to work under field conditions in terms of operational parameters, process design, climate (e.g. humidity, temperature, wind), air quality and the presence of particles. Unlike a laboratory-controlled experiment, a pilot study evaluates the efficacy of biofouling control strategies with more representativeness. For five weeks the three pilot-scale CTs were monitored and subjected to SWRO permeate supplemented with different nutrient dosages to (1) investigate the impact of limiting nutrients (C and P) on biofilm formation, (2) evaluate the changes in biofilm composition throughout the system and (3) assess the potential of low-nutrient content feed water against CT biofouling.

Materials and methods

Pilot set-up

System operation

The pilot facility is located at the central utility plant of King Abdullah University of Science and Technology (KAUST) in Saudi Arabia. It consists of three identical parallel counter flow induced draft CT systems. The systems are shown in Figure 1, and the detailed information was described in a previous study (Al-Bloushi et al. 2017). In short, each CT unit has a total volume of 62 l, and a cooling capacity of 15 kW. SWRO permeate produced at the desalination plant in KAUST (Belila et al. 2016) was used as the feed water. The SWRO permeate was carried through a 40 m long plastic pipe to a buffer tank of $7\,m^3$. Three connected pipelines at the bottom of the buffer tank allowed the distribution of feed water to the three pilot CTs. Feed water valves were triggered when the water levels in the basin dropped, resulting in average flows between 25 and 35 l h^{-1} depending on the external temperature and humidity. Continuous blowdown water flows were set at 5 l h^{-1}, and maintained a cycle of concentration (COC) between 5 and 7. Temperature differences along the heat exchangers were kept between 6 °C and 10 °C with a cold temperature between 27 °C and 30 °C in the basin and a hot temperature between 32 °C and 37 °C after the heat exchanger. The operation of the pilot was controlled automatically with an online system monitoring the following parameters: flow rate, temperature and pH. In addition, the pH and conductivity of the collected water samples were measured manually using

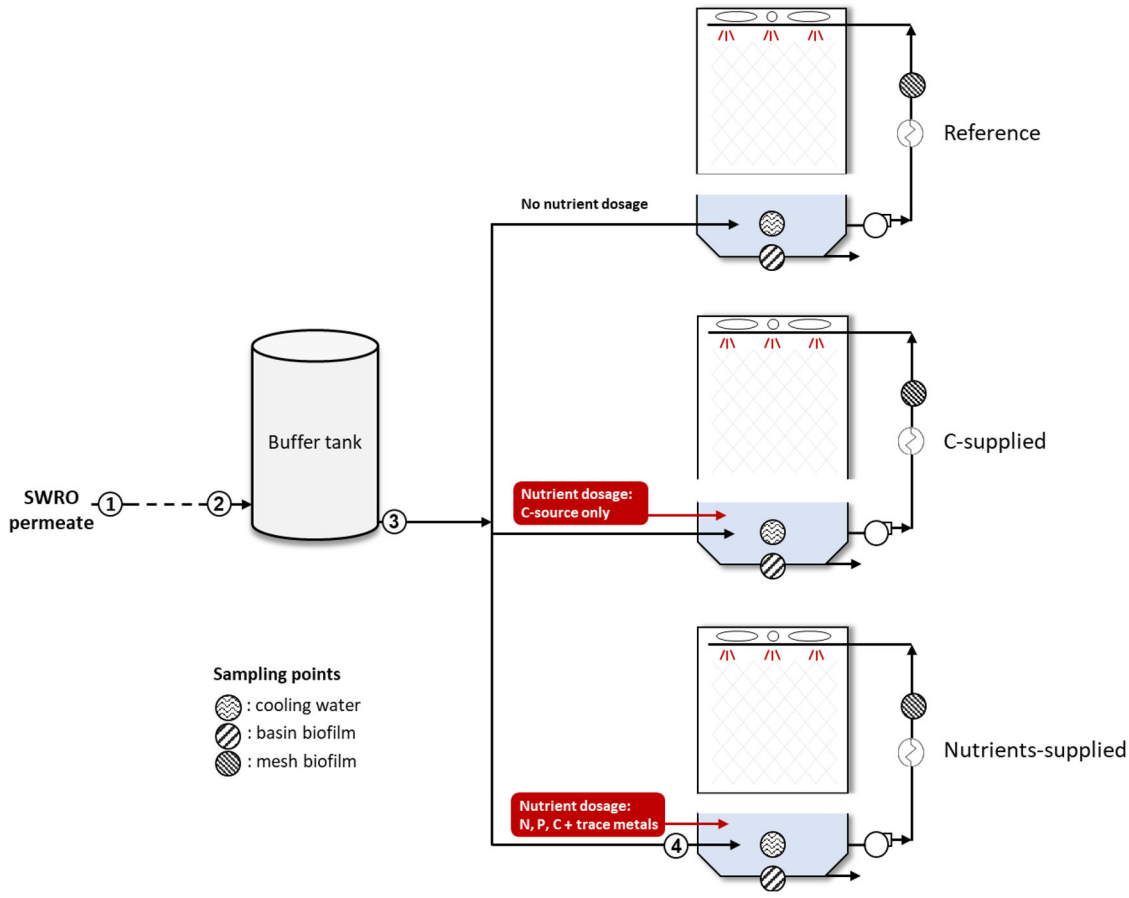

Figure 1. Scheme of the pilot installation. Seawater reverse osmosis (SWRO) permeate was used as source water. Acetate (C) was dosed in the C-supplied cooling tower and nitrate, phosphate and acetate (N, P, C) were dosed in the Nutrients-supplied cooling tower. In addition to the cooling tower samples, the water from locations 1 to 4 was collected for a water quality test.

Table 1. Nutrient dosages applied in the cooling towers.

Dosage	Reference	P-limited	Non-P-limited
Main elements	–	C	C, N, P
Compounds	–	Acetate	Acetate, nitrate, phosphate
Concentration in feed (μg l^{-1})	–	500	500, 100, 50
Trace metals	No	No	Yes (see Supporting Information Table S1)

a pH meter (Cyberscan pH6000, Eutech) and a conductivity meter (ProfiLine Cond3310, WTW). The pH values remained between 8.0 and 8.3, and conductivity values varied between 6 and 8 mS cm^{-1} in all CTs along the experiment. Cleaning of the systems was performed prior to the experiment as follows: (1) recirculation of sodium hydroxide solution (0.1 M) for 2 h; (2) flushing with SWRO permeate; (3) recirculation of hydrochloric acid solution at pH 2 for 2 h; (4) flushing with SWRO permeate.

Nutrient dosages

Nutrients were added to the CT basins to avoid bacterial growth inside the feed water pipelines. The following conditions were applied: (1) reference: without the addition of nutrient; (2) C-supplied: with a concentration of organic carbon of 500 μg $l^{-1}_{feed\ water}$; (3) nutrients-supplied: with concentrations of carbon, nitrogen and phosphorus (C, N, P) of 500, 100 and 50 μg $l^{-1}_{feed\ water}$, respectively, and trace metals (composition described in Supporting Information Table S1). The following sources were used for the C, N, P nutrients: sodium acetate trihydrate ($CH_3COONa{\cdot}3H_2O$; for a 'C' source), sodium nitrate ($NaNO_3$; for a 'N' source) and sodium phosphate monobasic monohydrate ($NaH_2PO_4{\cdot}H_2O$; for a 'P' source), all purchased in analytical grade from Sigma Aldrich. Table 1 and Supporting Information Table S1 summarize the compositions and dosing amounts of the nutrient solutions in each CT unit. All the

Table 2. Analyses of water parameters.

Parameter	Unit	Concentrations in feed water before nutrient dosages
Total phosphorus	µg l^{-1}	<20
Orthophosphate	µg l^{-1}	<10
TOC	mg l^{-1}	<0.3
COD	mg l^{-1}	<2

nutrient solutions were adjusted to pH 11 with the addition of NaOH prior to dosage, and the solutions were refreshed every two days to avoid bacterial growth in the nutrient solution containers.

Water quality analyses

Total phosphorus was analysed by inductively coupled plasma atomic emission spectroscopy (ICP-OES, Varian 720-ES). A standard curve was made with a phosphorus standard solution. 10 mL of water samples and standard solutions (20–500 ppb) which were made using a phosphorus standard solution (Inorganic Ventures) were prepared by adding 1% (v v^{-1}, final concentration) nitric acid. The total phosphorus concentration was calculated based on the standard curve. Orthophosphate concentration was measured with a low detection auto analyser using a colorimetric based method (SEAL AutoAnalyser 3 HR, Seal Analytical) following the proposed protocol by Murphy and Riley (1962). Total organic carbon (TOC; Table 2) was analysed using a TOC analyser (TOC-L CSH, Shimadzu Corporation) after filtration through a 0.45 µm pore size sterile PVDF syringe filters. Chemical oxygen demand (COD) was measured using a Hach TNT plus COD test kit and measured with a Hach spectrophotometer (DR 3900, Hach). Trace metal concentrations were analysed by inductively coupled plasma mass spectrometry (ICP-MS; Agilent 7500CX, Agilent).

Bacterial growth potential

Identification of limiting nutrient in cooling waters

The methodology applied for determining the limiting nutrient was derived from Prest et al. (2016). Bacterial growth potential tests were performed in sterile containers. Recirculating water samples from the three CTs were collected onsite and immediately filtered through a 0.45 µm pore-size sterile nylon syringe filter (Sartorius) to avoid predation by higher organisms such as protozoa. Each sample was split into ten aliquots of 30 ml. The same nutrient compounds as dosed in the CTs were added to the aliquots as follows: no addition ('Blank'), 1 mg-N + trace elements ('N + M'), 1 mg-P ('P'), 2 mg-C ('C'), 2 mg-C + 1 mg-N + 1 mg-P + trace elements ('All'). The test was performed in duplicate ($n = 2$). The aliquots were incubated at 37 °C in the dark with no shaking. Bacterial growth was monitored daily using a BD Accuri™ C6 flow cytometry (BD Biosciences) by staining with SYBR Green I (10,000 ×; Invitrogen). The final concentration of SYBR Green I in the samples was 1.96 µM. The staining protocol and flow cytometry analysis are described in the literature (Hammes et al. 2008; Prest et al. 2016). The incubation period was five days, after which the stationary phase was reached in all aliquots. The net growth was calculated by subtracting the cell count on day 0 from the cell count on day 5 for each growth test.

Growth potential of the feed water

The glass vessels used in this incubation test were soaked overnight in 0.2 M HCl solution, rinsed with deionized water and placed in an oven at 450 °C for 4 h to remove AOC residues. Samples of 100 ml from the sampling locations 1 to 4 shown in Figure 1 (1: SWRO permeate, 2: buffer tank inlet, 3: buffer tank outlet, 4: CT feed) were collected and incubated in the dark at 37 °C for five days. Total cell numbers were monitored using a BD Accuri™ C6 flow cytometry (BD Biosciences). The staining protocol with SYBR Green I (10,000 ×; Invitrogen) and flow cytometry analyses were as described in previous papers (Hammes et al. 2008; Prest et al. 2016).

Collection of deposit samples

Deposits consisting of biofilm and sediment accumulation were collected from the recirculation line and basin of each CT unit (Figure 1) at the end of the experiment after the water was drained from the system. Pieces of deposit (4 cm × 4 cm) from each basin floor were collected for quantification of dry-ash, ATP and chlorophyll, EPS extractions and 16S/18S rRNA gene amplicon sequencing. To sample each recirculation line, three stainless steel mesh coupons (Imotron) were inserted in a corrosion rack prior to the start of the experiment. The corrosion racks were located after the heat exchangers, in the heated water stream of each CT. The coupons were collected after the 5-week experiment to analyse the accumulated material in terms of wet weight, ATP quantification and 16S/18S rRNA gene amplicon sequencing.

Biofilm analytical methods

Dry-ash

The wet weight of fresh deposit samples was measured using a high precision analytical balance. For the dry mass, basin deposit samples were spread over a disposable aluminium foil cup to allow optimal contact with air. The samples were heated at 80 °C until no further water loss was measured. Dried samples were then transferred to crucibles, and the ash-free dry weight for the accumulated organic content was obtained after dry ashing at 500 °C for 4 h. The measurements were performed in triplicate.

ATP measurements

For each CT, one mesh coupon and one piece of fresh basin deposit (4 cm × 4 cm) were collected in 50 ml sterile centrifuge tubes (Greiner) containing 30 ml of NaCl 0.85%. The tubes were vortexed at maximal speed for 5 min and sonicated using an ultrasonic homogenizer (Qsonica sonicators) for 1 min with the following settings: output power 15 W and frequency 20 kHz. The homogenized solutions were subsequently filtered through a 0.45 µm pore-size sterile filter (Sartorius). ATP measurements were performed in duplicate with an ATP analyser (Advance™, Celsis) according to the manufacturer's protocols.

Extraction of extracellular polymeric substances

Triplicate deposit samples from the CT basins were frozen at −80 °C and lyophilized (Alpha 1-4 LDplus, Martin Christ) prior to the extraction. EPS were extracted at high temperature in alkaline conditions, following a method adapted from (Felz et al. 2016). In brief, 0.5 g of freeze-dried samples were stirred in 50 ml of 0.1 mol l^{-1} NaOH at 80 °C for 30 min. The containers were placed in ice water for 3 min to stop the extraction. Cooled mixtures were centrifuged at 3,300 × *g* at 4 °C for 30 min. The supernatants were dialyzed overnight (SnakeSkin 3.5 K MW, Thermo Fisher Scientific), frozen at −80 °C and lyophilized.

Quantification of phosphorus in EPS

For phosphorus quantification, 3 mg of lyophilized EPS were solubilized in 5 ml of ultrapure water. The total phosphorus content was determined with a HACH spectrophotometer (DR3900, Hach Lange) using the Hach Lange LCK 349 cuvette test kit (HACH).

Functional groups of EPS

The Fourier transform infra-red (FTIR) spectrum of the lyophilized EPS was performed on a FTIR Spectrophotometer (Perkin-Elmer) at room temperature, with a wavenumber range from 500 cm^{-1} to 4,000 cm^{-1}. A resolution of 4 cm^{-1} and an accumulation of eight scans were applied on each sample.

Chlorophyll measurements

Quantification of chlorophyll *a* and *b* (chlorophyll *a* + *b*) was conducted following the proposed protocol from Caesar et al. (2018). In brief, each basin biofilm sample was dried at 60 °C for 24 h before analysis. One gram dry weight of sample was placed in a 15 ml screw-cap glass vial, followed by a spatula tip of $CaCO_3$ and 6 ml of dimethyl sulfoxide (DMSO) (Sigma Aldrich). The vial was placed in a water bath at 65 °C for 90 min. After the first extraction cycle, the supernatant was transferred to a new vial. Another 6 ml of DMSO were added to the initial vial containing the biofilm and a second extraction was performed at 65 °C for 90 min. The supernatants from the first and second extractions were combined and centrifuged for 10 min at 3,000 × *g*. The absorbance was measured using a UV–Vis spectrophotometer (Lambda 45, Perkin-Elmer) at 648, 665 and 700 nm. The equations for the calculation of the amount of chlorophyll *a* and *b* are described elsewhere (Caesar et al. 2018).

Microbial communities in the water and deposit samples

Cooling water samples of 2.4 l were collected and filtered on 0.2 µm pore sized mixed cellulose esters membrane (GSWP04700; Millipore). Deposits from one mesh coupon and from the basin floor of each CT were collected and frozen at −20 °C until DNA extraction. Genomic DNA was extracted using a DNeasy PowerWater kit (Qiagen) according to the manufacturer's instructions. As an additional step, samples in the lysis buffer were heated at 65 °C for 10 min. The DNA concentration was quantified using a Qubit dsDNA high sensitivity (HS) or Qubit broad range (BR) assay kit (Life Technologies). The extracted DNA was stored at −80 °C until further analysis. Eukaryotic communities were analysed by DNASense ApS in Aalborg with 18S rRNA gene amplicon sequencing targeting the eukaryotic variable region V4 (position 571–980). The following forward and reverse tailed primers were used: [571F] 5′-GCCGCGGTAATTCCAGCTC-3′ and [980R] 5′-

CYTTCGYYCTTGATTRA-3′. Bacterial communities were analysed by DNASense ApS with amplicon sequencing of the 16S rRNA gene targeting the variable region V4 (position 515-806). The following forward and reverse tailed primers were used: [515F] 5′-GTGYCAGCMGCCGCGGTAA-3′ and [806R] 5′-GGACTACNVGGGTWTCTAAT-3′. Samples were paired-end sequenced (2×300 bp) on an Illumina MiSeq instrument using the MiSeq Reagent kit v3 (Illumina). >10% PhiX Control v3 Library was added as a spike-in to overcome low nucleotide diversity. The reads were trimmed for quality, clustered and operational taxonomic unit (OTU) were generated based on 97% similarities using USEARCH. Taxonomy was assigned using QIIME, with a confidence of 0.8, and the SILVA database. Biological duplicates of the basin deposit and cooling water of each CT were analysed. The DOI of the raw sequencing data is indicated in Supplementary materials. The bacterial and eukaryotic communities are described in Figure 5 and Supporting Information Figures S5 and S6 and Tables S2 and S3. Principal component analyses (PCA) comparing bacterial community structures and eukaryotic community structures were performed on the OTUs generated and their abundance with the Bray-Curtis matrix using the software Mothur v.1.40.5. PCA charts displayed in Figure 6 and Supporting Information Figure S8 indicate a high similarity in community structures of the samples clustering together.

Results

Determination of the limiting nutrient in the cooling tower waters

Growth potential tests were used to identify the bacterial growth limiting compound in each CT (Figure 2). A similar approach has been applied for determining the limiting nutrients in drinking water distribution networks (Prest et al. 2016). In the reference CT and CT supplied with carbon (Figure 2a and b), higher net bacterial growth occurred with the addition of phosphorus (P) to the water aliquots ($5.9 \pm 0.4 \times 10^6$ cells ml^{-1} and $8.1 \pm 0.4 \times 10^6$ cells ml^{-1}, respectively). In contrast, the addition of nitrogen with trace metals (N + M) and carbon (C) did not promote bacterial growth. The growth of microorganisms in the reference and the carbon supplied CTs was, therefore, primarily limited by phosphorus. In the CT enriched with all nutrients (Figure 2c), the high initial concentration of C, N and P supplied with the feed water caused a significant net cell growth in the blank aliquots ($5.7 \pm 0.7 \times 10^6$ cells ml^{-1}). Further addition of N + M and P had a negligible impact on cell growth compared with the addition of a C source ($21.2 \pm 1.8 \times 10^6$ cells ml^{-1}), indicating that organic carbon was the primary limiting compound. CTs were, therefore, operated with different limiting compounds, either carbon or phosphorus. These differences could affect the selection and metabolism of

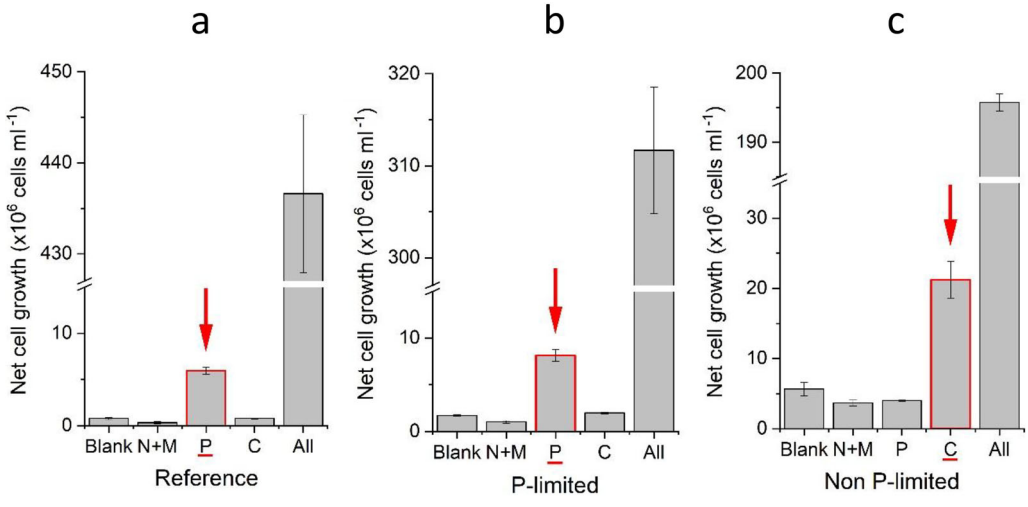

Figure 2. Determination of the limiting nutrient in the three cooling tower systems supplied with (a) RO permeate only, denoted as 'Reference'; (b) RO permeate enriched in carbon source, denoted as 'P-limited'; and (c) RO permeate enriched in all nutrients, denoted as 'Non P-limited'. Elements were added in cooling water samples as follows: no addition (Blank), nitrogen + trace metals addition (N + M), phosphorus (P), carbon (C), all nutrients (All). The error bars indicate the error on duplicate samples for each condition. The red arrows indicate the limiting nutrient in the corresponding cooling tower: phosphorus in (a) and (b) and carbon in (c).

the microorganisms, and thereby the biofouling potential in the processes.

In the remaining part of the manuscript, the CT (1) not supplied with nutrient, is denoted as 'Reference'; (2) supplied with carbon only, is denoted as 'P-limited'; and (3) enriched in all nutrients, is denoted as 'Non-P-limited'.

Deposit formation in the cooling towers

Macroscopic description

Deposits were collected from the basin floor, and the mesh coupons were retrieved from the recirculation line after operation for five weeks. The visual appearance of the accumulated material in the basin (Supporting Information Figure S1) varied markedly between the three CTs. The reference CT displayed limited growth, mostly an accumulation of sediment forming a sludge-like layer. In the P-limited CT, fed with carbon enriched feed water, an extensive deposit layer of 3 to 5 mm thick was formed with high structural integrity, homogeneously spread and covering the entire floor of the basin. Unlike the others, the P-limited layer could be removed from the surface as one piece when manually taken out. The non-P-limited CT showed extensive and non-homogeneous deposit on the bottom surface with visible growth of phototrophic organisms. Results from the dry-ashing showed that the deposits from all basins contained between 40 and 60 mg cm^{-2} of sediment, mainly silica from sand particles carried by the wind or sandstorms, and other inorganic compounds.

The mesh coupons collected from the recirculation lines had a similar appearance, with brown deposits suggesting a combination of biofilm and sediment (Supporting Information Figure S2). Accumulated matter on the mesh coupons from the P-limited and non-P-limited CTs was considerably higher than on the reference CT coupon. Even so, the presence of accumulated material in the reference CT was unexpected since RO permeate was used as feed water with no additional dosage.

Overall, the changes in nutrient dosages caused different morphologies and varied thicknesses of biofilm layers in the CT basins. The presence of sediments confirmed the high sensitivity of the CT systems to the accumulation of materials introduced by the air flow.

Compositions of basin biofilms

In the reference CT, 3.22 ± 0.69 mg cm^{-2} of organic matter (Figure 3a) had accumulated on the basin floor. In the CT operated with carbon enriched feed water, P-limited, the amount of accumulated organic matter was 7.30 ± 0.38 mg cm^{-2} while the nutrient containing feed water, non-P-limited, resulted in an accumulation of 6.14 ± 1.49 mg cm^{-2}. P-limited and non-P-limited CTs showed significantly higher organic matter accumulation than the reference (p-values $< .01$ based on Z-score values). However, the difference between P-limited and non-P-limited was not significant (p-value $> .05$). The larger standard deviation illustrates the uneven biofilm layer of the non-P-limited CT basin.

ATP quantification indicated a very low active biomass concentration in the reference and P-limited biofilms (< 10 ng g^{-1} organic matter) compared with the non-P-limited samples ($2.6 \pm 0.1 \times 10^3$ ng g^{-1} organic matter) (Figure 3b). The results suggest that under phosphate limitation, microbial growth was indeed limited, but the abundant accumulation of organic matter still occurred in the presence of easily assimilable carbon. The percentage of extracted EPS in the different samples, however, were all very similar to values ranging between 20 and 30% (w w^{-1}) of the organic matter (Figure 3c). A relatively higher phosphorus content (Figure 3d) was observed in the EPS of the non-P-limited CT ($0.62 \pm 0.02\%$ compared with $0.37 \pm 0.06\%$ and $0.35 \pm 0.01\%$ in the reference and P-limited). The FTIR spectra (Supporting Information Figure S3) of the extracted EPS display the characteristic carbohydrate band at 940–1,200 cm^{-1} (Zhu et al. 2012; Boleij et al. 2019) and protein band at 1,500–1,700 cm^{-1} with amide I and amide II corresponding peaks (Barth 2007). The ratio of the intensity of the protein band compared with the carbohydrate band is lower in the reference and P-limited samples than in the non-P-limited sample, indicating a preference for carbohydrate production rather than protein when phosphorus is limited. In addition, chlorophyll a and b measurements (Supporting Information Figure S4) correlate with visual observation with a considerably higher concentration in the non-P-limited conditions than in the reference and P-limited conditions (respectively 40, 3 and 19 μg g^{-1} basin deposit).

Compositions of deposit layers on the mesh coupons

Deposit mass and ATP were also quantified from the mesh coupons placed in the recirculation pipe (Figure 4). The mesh coupon from the reference system reached only 28 ± 3 mg cm^{-2} of accumulated

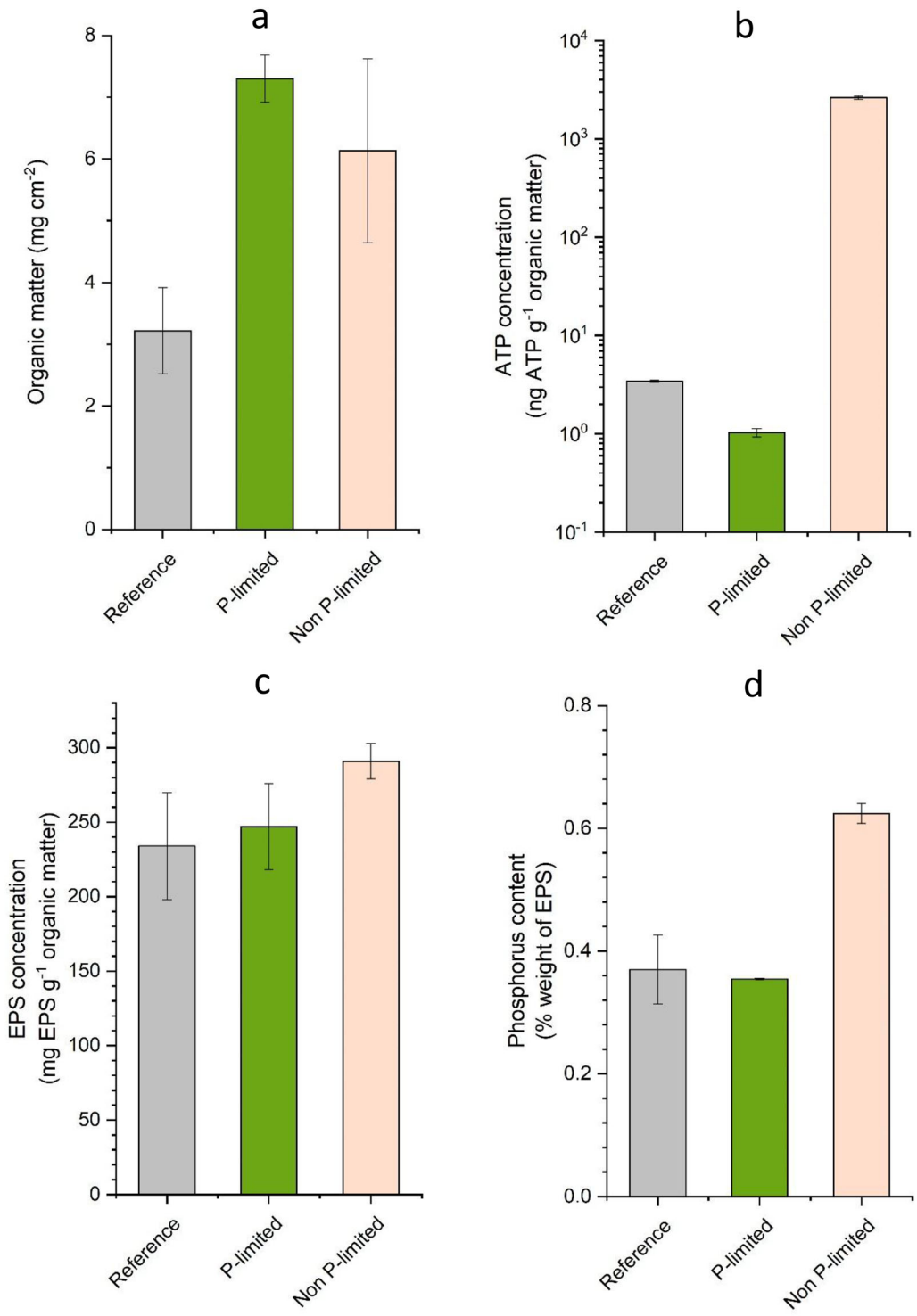

Figure 3. Amounts of organic matter (a), ATP concentrations (b), EPS concentrations (c) and phosphorus content in the EPS (d) in the basin deposits.

material, significantly less than on the coupons from the P-limited and non-P-limited CTs (p-values $<$ .0001), which had accumulated 50 ± 5 mg cm^{-2} and 49 ± 4 mg cm^{-2}, respectively. The mesh coupon deposit from the non-P-limited CT contained a significantly higher active biomass concentration (43 ng ATP g^{-1} wet deposit) than deposits from the reference and P-limited CTs (5 and 2 ng ATP g^{-1} wet deposit). The results for biomass growth in the CT basin and on the coupons in the recirculation pipe

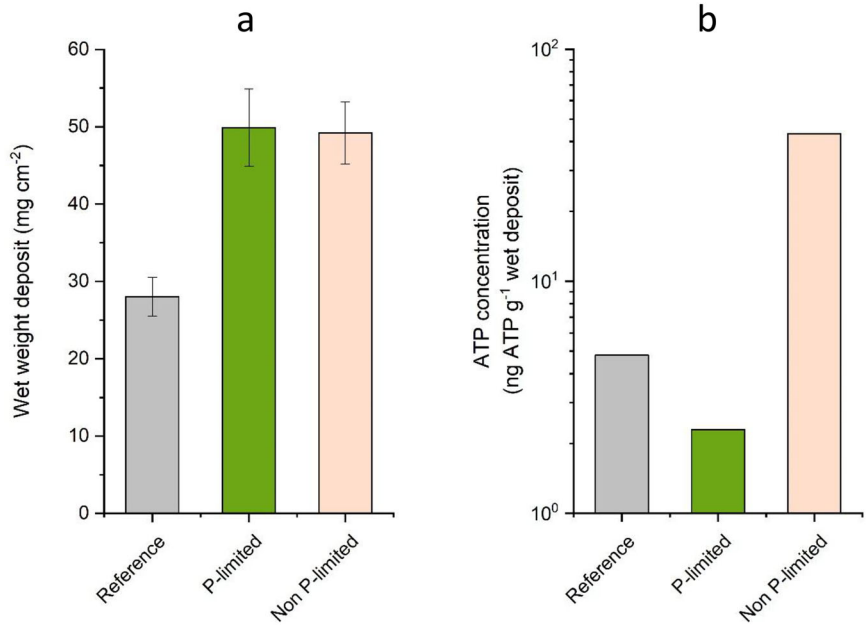

Figure 4. Deposit wet weights (a) and ATP concentrations (b) on the mesh coupons located in the recirculation line, after the heat exchanger.

are congruent, suggesting that biofouling occured consistently along the process, i.e. basin and recirculation pipe.

Changes in microbial community structures

Bacterial community and diversity analyses (Figures 5 and 6) provided more in-depth details on the collected biomass and allowed visualization of the changes depending on location in the system and nutrient availability. The bacterial community composition at the phylum level (Figure 5) showed similarity based on the locations of the samples. Cyanobacteria had relatively high abundances in the basin deposits (23, 36 and 43% of 16S rRNA gene reads in the reference, P-limited and non-P-limited CTs respectively) due to the exposure to sunlight during daytime. They were in lower abundances in the water samples (4, 7 and 15%) and negligible in the mesh deposits located in the dark (<2%). Proteobacteria was clearly the main water sample phylum with 66, 69 and 60% while Bacteroidetes, Planctomycetes and Proteobacteria were more evenly represented in the mesh deposits. The most abundant bacterial genera and a bar chart of the community composition at the family level in each sample are given in Supporting Information (Figure S5 and Table S2).

Principal component analysis (Figure 6) displays the similarity in bacterial community structures of samples based on the generated OTUs and their abundances. The principal components PC1 and PC2 showed 29.3 and 19.5% of the variation, respectively. In each CT, the water, mesh and basin biofilm samples diverge from each other, confirming that a bacterial selection occurred within the biofilms due to the local environmental conditions (e.g. exposure to sunlight and temperature), resulting in a distinct microbiome from the water phase. Interestingly, the limitation in phosphate seems to have caused an additional distinction. The plot shows clustering between the reference and non-P-limited CT samples but divergence of the P-limited CT samples. P-limitation caused a switch in bacterial community structure while the enrichment in all nutrients (C, N and P) promoted bacterial growth but did not seem to strongly affect the community structure when compared with the reference.

Deterioration in water quality along the feed water line

Due to the observation of biofilm accumulation in the reference CT operated with SWRO permeate, it was decided to investigate the stability of the feed water quality along the line between RO installation and CTs. Measured water quality parameters, viz. total organic carbon (TOC), chemical oxygen demand (COD) and total phosphorus concentrations, were all below the quantification limit (Table 2). A bacterial incubation test was performed to determine the

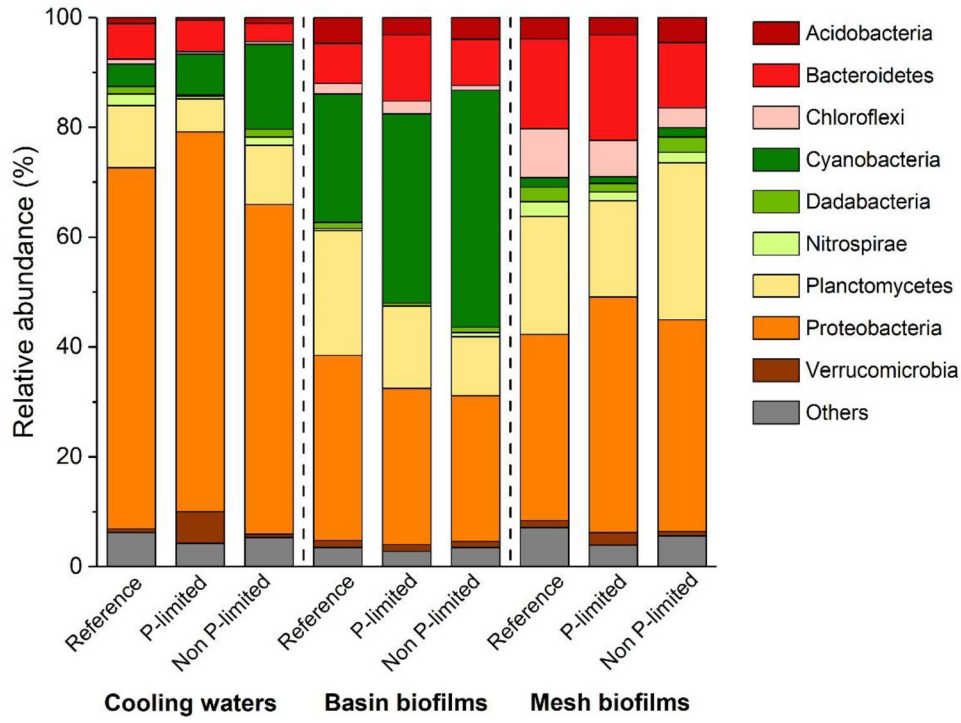

Figure 5. Relative abundance of bacterial communities at the phylum level in the cooling water and deposit samples (in percentage of 16S rRNA gene reads). The abundance of Cyanobacteria constitutes the main difference between the basin and mesh biofilms, while cooling waters were dominated by the phylum Proteobacteria. 'Others' contains bacterial phyla of <1% abundance in all samples.

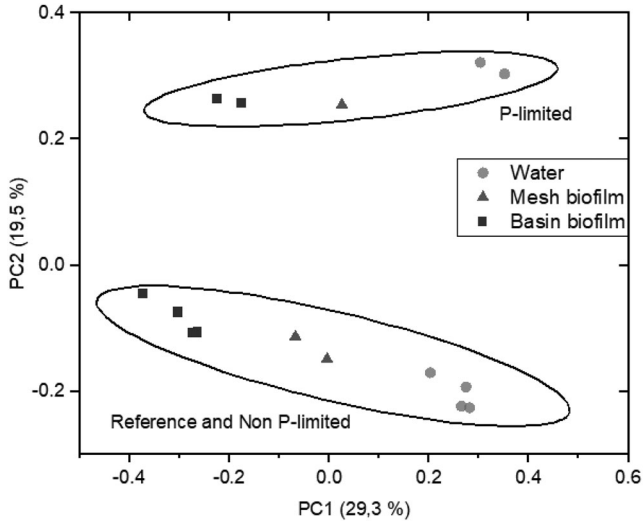

Figure 6. Principal component analysis (PCA) comparing the bacterial community structure of the waters, mesh biofilms and basin biofilms. The circles indicate that the P-limited cooling tower samples diverged from the reference and non-P-limited cooling towers. Additionally, the three sampling locations diverged from each other. The waters and basin biofilms were analysed in duplicate.

potential impact of the pipes and buffer tank on the feed water quality before supply to the CTs.

Samples from the feed water line were collected at four locations according to the numbering in Figure 1: SWRO permeate, buffer tank inlet, buffer tank outlet and CT feed. Each sample was incubated in the laboratory, and the total bacterial cell count was monitored over five incubation days. As shown in Figure 7, samples already displayed higher cell counts on collection day (day 0) in the buffer tank outlet and in the CT feed ($61.9 \pm 0.7 \times 10^3$ and $90.3 \pm 0.6 \times 10^3$ cells ml^{-1}) compared with the buffer tank inlet ($3.2 \pm 0.1 \times 10^3$ cells ml^{-1}). The difference in total cell numbers between the inlet and outlet of the buffer tank can be attributed to the retention time of around one day of the RO permeate in the tank. After incubation of the samples for five days, a higher cell count was reached in the last sampling location, CT feed (2.7×10^5 cell ml^{-1}). The daily total cell counts are shown in Supporting Information Figure S8. These results indicate that the pipe and buffer tank of the feed water line contributed to cell growth through organic carbon leaching from the surface materials to the water phase. Even though the tank and pipes were extensively cleaned before the start of the experiments, the high-quality SWRO permeate was deteriorated substantially by the installation and surrounding environments (e.g. temperature, wind and sunlight). As a result, no conclusion can be drawn on the efficiency of the SWRO permeate as feed water for CTs due to quality deterioration. However, the study

illustrates the difficulty of maintaining clean installations at an industrial scale to avoid any contamination.

Discussion

P-limitation restricts microorganism growth but not biofilm formation in cooling tower systems

A goal of this study was to investigate the efficiency of phosphate limitation as a preventive method for biofouling control in CTs. The applied short-term approach, based on nutrient dosages in the feed water, has been shown to be suitable for prediction of long-term biofouling (Sanawar et al. 2017) and has been used to study membrane filtration systems (Siddiqui et al. 2017; Sanawar et al. 2018). The pilot-scale experiment showed that: (1) active biomass growth in the CT was strongly inhibited under P-limited conditions compared with conditions with additional phosphate supplied (Figures 3 and 4); (2) the overall accumulation of organic matter was similar when all nutrients were supplied or under P-limited conditions with only organic carbon supplied (Figure 3); (3) P-limitation caused a shift in bacterial community structure (Figure 6) and seemed to promote the production of carbohydrates over proteins by the microorganisms in the extracellular matrix and to result in a more homogeneous biofilm (Supporting Information Figures S1 and S3).

Phosphorus limitation in the cooling water affected microbial growth and the composition of the EPS but was not efficient against biofouling in the presence of high AOC. The availability in carbon was, therefore, the main factor determining the extent of biofilm growth.

The necessity of phosphorus for microbial growth has been extensively described in the literature (Holtan et al. 1988; Smith and Prairie 2004; He et al. 2018). The molar ratio between C:N:P in microbial biomass has been approximated to 100:20:1.7 (Tchobanoglous and Burton 1991). At a low enough concentration, phosphorus can then become a limiting nutrient for cell growth. According to mixed and pure culture studies, phosphate limitation has been shown to cause selection of microbial communities (Keinänen et al. 2002; Samaddar et al. 2019) and to induce changes in cell physiology, such as degradation of polyphosphate or exchange of phosphorus-free membrane lipids, by affecting their metabolism (Romano et al. 2015).

There are, however, diverging opinions regarding the impact of low phosphorus on biofilm formation. Some authors report strongly inhibited biofilm formation under P-limited conditions (Vrouwenvelder et al. 2010; Kim et al. 2014). Other authors indicate higher EPS production by cells resulting in a low population but an extensive and homogeneous biofilm with a gel-like structure (Hoa et al. 2003; Fang et al. 2009; Li et al. 2016; Desmond et al. 2018). In the studies on phosphate quantification, the concentrations in the P-limited conditions were reported to be below the detection limit of the method applied, the lowest being 0.01 mg P l^{-1}. It is, therefore, a possibility that the phosphate concentrations in the studies from Vrouwenvelder et al. (2010) and Kim et al. (2014) were lower than in the studies where abundant biofilms were produced, although absolute values are lacking. The present results support previous observations that P-limitation inhibits cell growth but causes higher accumulated organic matter per active biomass unit. In other words, reaching P-limited conditions is not enough to avoid biofouling when there is still AOC in the system. Essentially, a complete absence of phosphate would be needed for biofouling prevention, which is difficult to achieve in open systems exposed to external conditions as is the case with CTs.

Under P-limitation, the transition to a more carbohydrate-dominated EPS structure was observed, compared with non-P-limited conditions (Supporting Information Figure S3). Native biofilm, i.e. during initial and irreversible attachment, is likely based on a high fraction of proteins due to the essential role of cell surface proteins in the attachment to the substratum, motility and surface colonization (Fong and Yildiz 2015). Nonetheless, when P is the primary limited compound, a shift in carbon metabolism can occur during biofilm maturation, and polysaccharide synthesis can be seen as an overflow metabolism induced by growth limitation (Russell and Cook 1995; Hessen and Anderson 2008). Similar observations have been made in studies of drinking water and wastewater bacterial biofilms (Hoa et al. 2003; Fang et al. 2009) and in diatoms (Brembu et al. 2017). When cell division becomes hindered, the synthesis of proteins and membrane lipids is strongly reduced as cells promote the production of extracellular polysaccharides over the synthesis of cell components and energy production.

Regarding the yield of extracted EPS, a higher EPS content in the accumulated organic matter in the P-limited sample would be expected compared with the non-P-limited sample since active biomass was strongly inhibited. It is important to note that limitations remain regarding the efficiency of the EPS extraction method. The choice was made to use an alkaline extraction at high temperature to improve the solubilisation of the structural EPS matrix and collect

a substantial fraction of the extracellular polymers (Felz et al. 2016). However, such extreme conditions can also cause loss of cell integrity and release of intracellular compounds (Seviour et al. 2019) while not extracting the matrix components totally. The higher phosphorus content in the non-P-limited extracted EPS might be caused by a higher extracellular DNA concentration and also the possible release of intracellular DNA occurring with cell lysis. The presence of intracellular material and the integrity of the cells with this EPS extraction method should be further investigated.

Comparison of biofilm microbial composition along the cooling tower system

Biofilms from full-scale CTs are generally collected from the wall of the CT basins, which is the most accessible location of the system and does not require interruption of operation (Di Gregorio et al. 2017). The present pilot study is the first describing analyses of microbial communities from different locations in the recirculation line of a nondisinfected CT.

The results from basin and mesh biofilms for each of the conditions tested were congruent regarding the extent of accumulated organic matter per active biomass (Figures 3 and 4). Yet, these results showed: (1) a divergence of bacterial communities compared with the water sample (Figure 6) and (2) variations in terms of the phototrophic organisms' content and the structure of the deposit (Supporting Information Figures S1 and S4).

Previous investigations of full-scale water processes and distribution networks have shown divergences in planktonic bacterial communities with sessile communities and indicated a higher richness in biofilm species (Keinänen et al. 2002; Wang et al. 2013; Di Gregorio et al. 2017). Changes are usually attributed to the attachment abilities of the microorganisms during the colonization phase. Indeed, bacteria able to produce adhesion proteins and pili or containing lipopolysaccharides on the outer layers would be favoured and initiate biofilm formation (Walker et al. 2004; Hori and Matsumoto 2010; Conrad 2012). Planktonic microorganisms, therefore, play the role of inoculant from which bacteria selectively attach to the substratum. The attached bacterial community further evolves independently from the water microbiome. The principal component analysis supports this assumption with the biofilm community structures from two locations in the system (basin and recirculation line after heat exchanger) deviating from the water community structure. As described in other reports, the water community was majorly constituted of Proteobacteria (Wang et al. 2013; Tsao et al. 2019), while bacterial phyla were more evenly represented in biofilm communities. In addition, the divergence between the community structures of the basin and mesh biofilms for each condition suggests that the biofilm communities vary along the system and that samples from the basin biofilm only are not representative of other locations, e.g. heat exchangers in the CT. The deviation is partially driven by the presence of phototrophic organisms (Figure 5 and Supporting Information Figure S4) in the basin following intense light exposure (Di Gregorio et al. 2017) and can be amplified by additional factors such as the difference in temperature and substratum (Hancock et al. 2011). The presence of phototrophs may worsen biofilm development through fixation of CO_2 from the atmosphere contributing to the accumulation of organic matter (Roeselers et al. 2008; Rossi and De Philippis 2015). Phototrophic mats have been largely described as multilayer ecosystems (Ward et al. 1998; Guerrero et al. 2002; Roeselers et al. 2007). Such structures were observed in the basins of the CTs, especially under P-limited condition, with a homogeneous surface layer and non-P-limited condition with a more disparate biofilm arrangement (Supporting Information Figure S1). These findings point to the importance of sampling location when studying the CT biofilm microbiome.

Implications of the study for industrial cooling tower systems

As described previously, phosphorus removal from the feed water could have an undesirable effect and aggravate biofilm formation if the remaining concentration is not low enough. Its limitation has been shown to induce greater EPS production by the cells and to result in a homogenous structural deposit, detrimental for full-scale processes. Total removal of phosphorus from a water source is hardly achievable, and phosphorus-based corrosion inhibitors would have to be replaced by phosphorus-free products for the protection of the heat exchangers (Sandu et al. 2016; Wang et al. 2016). The intensive contact between water, ambient air and particles in the CT as well as evaporation are all factors that can also raise the element concentration in the system (Mahowald et al. 2008; Katra et al. 2016). Following the outcome of this study, removal of AOC seems to be a better approach than phosphorus removal to delay the formation of biofilm.

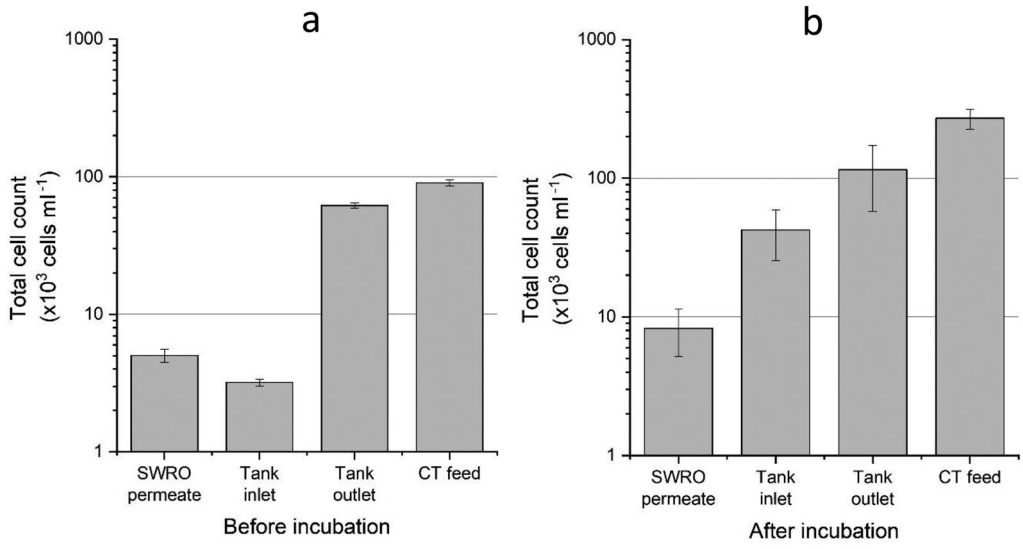

Figure 7. Cell count before (a) and after (b) incubation of water samples along the feed water pipe. Samples were collected from (1) the SWRO permeate, (2) the buffer tank inlet, (3) the buffer tank outlet and (4) the cooling tower feed as shown in Figure 1.

A growth potential measurement of the feed water was carried out to evaluate the SWRO permeate quality along the line. This approach has been previously applied to evaluate the biological stability of waters (Prest et al. 2016; Farhat et al. 2018a, 2018b). The results showed a leaching of nutrient along the pipes and reservoir, resulting in higher bacterial cell growth (Figure 7), and therefore, compromising the assessment of the SWRO permeate as CT feed water. This study was exposed to some difficulties related to the industrial scale of the set-up that are not usually considered during laboratory scale experiments, that is to say the impact of the onsite distribution system and effect of external conditions. Therefore, a conclusion could not be made on the suitability of the SWRO permeate as cooling water, but advice and suggestions for future work on industrial CTs can be drawn from the results obtained. The data illustrate the low feasibility of maintaining a sufficiently high feed water quality against biofouling in industrial cooling systems. As CTs are long-established systems, their feed water lines impact the quality of the water. For use as feed water, the RO installation should be located directly next to the cooling water system to have negligible contact time with the pipe surfaces, or the feed water line should be replaced prior to the change of water supply and made of non-leaching materials.

Conclusions

This pilot-scale study on the impact of nutrient availability on biofilm formation combined with an efficiency assessment of seawater reverse osmosis permeate as feed water in open recirculating cooling towers (CTs) showed that P-limitation restricts the growth of microorganisms but not biofilm formation in CT systems. The study underlines the significant risks of (1) water quality deterioration by the feed water line and (2) contamination from the environment of cooling water in open recirculating CTs. A higher C:P ratio was shown to affect the bacterial community structure and seemed to promote the production of carbohydrates over proteins. In each CT, biofilms from the basin and coupons in the recirculation pipe diverged from each other and from the water phase in terms of bacterial community structure. The biofilm microbiome, therefore, develops independently from the planktonic microbiome and adapts to local conditions.

These research outcomes provide a basis for understanding biofilm growth factors in open recirculating CTs and contribute to the industrial field in the selection of feed water type and pre-treatments for CTs. Evaluation of the RO permeate as feed water to avoid biofouling requires further investigation and may be addressed in future studies.

Acknowledgements

The research reported in this manuscript would not have been possible without the support of Evides Industriewater B.V. and of the Water Desalination and Reuse Center (WDRC) and Central Utility Plant of KAUST.

Disclosure statement

No potential conflict of interest was reported by the author(s).

ORCID

Ingrid S. M. Pinel http://orcid.org/0000-0002-7323-1745

References

Al-Bloushi M, Saththasivam J, Al-Sayeghc S, Jeong S, Ng KC, Amy GL, Leiknes T. 2018. Performance assessment of oxidants as a biocide for biofouling control in industrial seawater cooling towers. J Ind Eng Chem. 59: 127–133. doi:10.1016/j.jiec.2017.10.015

Al-Bloushi M, Saththasivam J, Jeong S, Amy GL, Leiknes T. 2017. Effect of organic on chemical oxidation for biofouling control in pilot-scale seawater cooling towers. J Water Process Eng. 20:1–7. doi:10.1016/j.jwpe.2017.09.002

Balamurugan P, Hiren Joshi M, Rao TS. 2011. Microbial fouling community analysis of the cooling water system of a nuclear test reactor with emphasis on sulphate reducing bacteria. Biofouling. 27:967–978. doi:10.1080/08927014.2011.618636

Barth A. 2007. Infrared spectroscopy of proteins. Biochim Biophys Acta. 1767:1073–1101. doi:10.1016/j.bbabio.2007.06.004

Belila A, El-Chakhtoura J, Otaibi N, Muyzer G, Gonzalez-Gil G, Saikaly PE, van Loosdrecht MCM, Vrouwenvelder JS. 2016. Bacterial community structure and variation in a full-scale seawater desalination plant for drinking water production. Water Res. 94:62–72. doi:10.1016/j.watres.2016.02.039

Boleij M, Seviour T, Wong LL, van Loosdrecht MCM, Lin Y. 2019. Solubilization and characterization of extracellular proteins from anammox granular sludge. Water Res. 164:114952. doi:10.1016/j.watres.2019.114952

Bradford SM, Palmer CJ, Olson BHJ. 1994. Assimilable organic carbon concentrations in Southern California surface and groundwater. Water Res. 28:427–435. doi:10.1016/0043-1354(94)90280-1

Brembu T, Mühlroth A, Alipanah L, Bones AM. 2017. The effects of phosphorus limitation on carbon metabolism in diatoms. Philos T R Soc B. 372:20160406. doi:10.1098/rstb.2016.0406

Caesar J, Tamm A, Ruckteschler N, Leifke AL, Weber B. 2018. Revisiting chlorophyll extraction methods in biological soil crusts–methodology for determination of chlorophyll a and chlorophyll a + b as compared to previous methods. Biogeosciences. 15:1415–1424. doi:10.5194/bg-15-1415-2018

Chen X, Stewart PS. 1996. Chlorine penetration into artificial biofilm is limited by a reaction – diffusion interaction. Environ Sci Technol. 30:2078–2083. doi:10.1021/es9509184

Conrad JC. 2012. Physics of bacterial near-surface motility using flagella and type IV pili: implications for biofilm formation. Res Microbiol. 163:619–629. doi:10.1016/j.resmic.2012.10.016

Daamen EJ, Wouters JW, Savelkoul JTG. 2000. Side stream biofiltration for improved biofouling control in cooling water systems. Water Sci Technol. 41:445–451. doi:10.2166/wst.2000.0478

De Beer D, Srinivasan R, Stewart PS. 1994. Direct measurement of chlorine penetration into biofilms during disinfection. Appl Environ Microbiol. 60:4339–4344. doi:10.1128/AEM.60.12.4339-4344.1994

Desmond P, Best JP, Morgenroth E, Derlon N. 2018. Linking composition of extracellular polymeric substances (EPS) to the physical structure and hydraulic resistance of membrane biofilms. Water Res. 132:211–221. doi:10.1016/j.watres.2017.12.058

Di Gregorio L, Tandoi V, Congestri R, Rossetti S, Di Pippo F. 2017. Unravelling the core microbiome of biofilms in cooling tower systems. Biofouling. 33:793–806. doi:10.1080/08927014.2017.1367386

Edwards M, Dudi A. 2004. Role of chlorine and chloramine in corrosion of lead-bearing plumbing materials. Am Water Works Ass. 96:69–81. doi:10.1002/j.1551-8833.2004.tb10724.x

Fang W, Hu JY, Ong SL. 2009. Influence of phosphorus on biofilm formation in model drinking water distribution systems. J Appl Microbiol. 106:1328–1335. doi:10.1111/j.1365-2672.2008.04099.x

Farhat N, Hammes F, Prest E, Vrouwenvelder J. 2018a. A uniform bacterial growth potential assay for different water types. Water Res. 142:227–235. doi:10.1016/j.watres.2018.06.010

Farhat NM, Loubineaud E, Prest EIEC, El-Chakhtoura J, Salles C, Bucs SS, Trampé J, Van den Broek WBP, Van Agtmaal JMC, Van Loosdrecht MCM, et al. 2018b. Application of monochloramine for wastewater reuse: effect on biostability during transport and biofouling in RO membranes. J Membr Sci. 551:243–253. doi:10.1016/j.memsci.2018.01.060

Felz S, Al-Zuhairy S, Aarstad OA, van Loosdrecht MCM, Lin YM. 2016. Extraction of structural extracellular polymeric substances from aerobic granular sludge. J Vis Exp. (115):54534. doi:10.3791/54534

Fong JNC, Yildiz FH. 2015. Biofilm matrix proteins. Microbiol Spectr. 3: 201–222.

Guerrero R, Piqueras M, Berlanga M. 2002. Microbial mats and the search for minimal ecosystems. Int Microbiol. 5: 177–188. doi:10.1007/s10123-002-0094-8

Hammes F, Berney M, Wang Y, Vital M, Köster O, Egli T. 2008. Flow-cytometric total bacterial cell counts as a descriptive microbiological parameter for drinking water treatment processes. Water Res. 42:269–277. doi:10.1016/j.watres.2007.07.009

Hancock V, Witsø IL, Klemm P. 2011. Biofilm formation as a function of adhesin, growth medium, substratum and strain type. Int J Med Microbiol. 301:570–576. doi:10.1016/j.ijmm.2011.04.018

He J, Wang W, Shi R, Zhang W, Yang X, Shi W, Cui F. 2018. High speed water purification and efficient phosphate rejection by active nanofibrous membrane for microbial contamination and regrowth control. Chem Eng J. 337:428–435. doi:10.1016/j.cej.2017.12.096

Hessen DO, Anderson TR. 2008. Excess carbon in aquatic organisms and ecosystems: physiological, ecological, and evolutionary implications. Limnol Oceanogr. 53: 1685–1696. doi:10.4319/lo.2008.53.4.1685

Hijnen WAM, Biraud D, Cornelissen ER, Kooij D. 2009. Threshold concentration of easily assimilable organic carton in feedwater for biofouling of spiral-wound membranes. Environ Sci Technol. 43:4890–4895. doi:10.1021/es900037x

Hoa P, Nair L, Visvanathan C. 2003. The effect of nutrients on extracellular polymeric substance production and its influence on sludge properties. Water SA. 29:437–442.

Holtan H, Kamp-Nielsen L, Stuanes AO. 1988. Phosphorus in soil, water and sediment: an overview. Hydrobiologia. 170:19–34. doi:10.1007/BF00024896

Hori K, Matsumoto S. 2010. Bacterial adhesion: from mechanism to control. Biochem Eng J. 48:424–434. doi:10.1016/j.bej.2009.11.014

Katra I, Gross A, Swet N, Tanner S, Krasnov H, Angert A. 2016. Substantial dust loss of bioavailable phosphorus from agricultural soils. Sci Rep. 6:24736. doi:10.1038/srep24736

Keinänen MM, Korhonen LK, Lehtola MJ, Miettinen IT, Martikainen PJ, Vartiainen T, Suutari MH. 2002. The microbial community structure of drinking water biofilms can be affected by phosphorus availability. Appl Environ Microbiol. 68:434–439. doi:10.1128/aem.68.1.434-439.2002

Kim C-M, Kim S-J, Kim LH, Shin MS, Yu H-W, Kim IS. 2014. Effects of phosphate limitation in feed water on biofouling in forward osmosis (FO) process. Desalination. 349:51–59. doi:10.1016/j.desal.2014.06.013

Lehtola MJ, Miettinen IT, Martikainen PJ. 2002. Biofilm formation in drinking water affected by low concentrations of phosphorus. Can J Microbiol. 48:494–499. doi:10.1139/w02-048

Li S, Wang C, Qin H, Li Y, Zheng J, Peng C, Li D. 2016. Influence of phosphorus availability on the community structure and physiology of cultured biofilms. J Environ Sci (China). 42:19–31. doi:10.1016/j.jes.2015.08.005

Mahowald N, Jickells TD, Baker AR, Artaxo P, Benitez-Nelson CR, Bergametti G, Bond TC, Chen Y, Cohen DD, Herut B, et al. 2008. Global distribution of atmospheric phosphorus sources, concentrations and deposition rates, and anthropogenic impacts. Global Biogeochem Cycles. 22. doi:10.1029/2008GB003240

Meesters K, Van Groenestijn J, Gerritse J. 2003. Biofouling reduction in recirculating cooling systems through biofiltration of process water. Water Res. 37:525–532. doi:10.1016/s0043-1354(02)00354-8

Melo LF, Flemming HC. 2010. Mechanistic aspects of heat exchanger and membrane biofouling and prevention. In: Zahid Amjad, editor. The science and technology of industrial water treatment. Abington, UK: Taylor and Francis Group; p. 365–380.

Miettinen IT, Vartiainen T, Martikainen PJ. 1997. Phosphorus and bacterial growth in drinking water. Appl Environ Microbiol. 63:3242–3245. doi:10.1128/AEM.63.8.3242-3245.1997

Murphy J, Riley JP. 1962. A modified single solution method for the determination of phosphate in natural waters. Anal Chim Acta. 27:31–36. doi:10.1016/S0003-2670(00)88444-5

Nguyen T, Roddick FA, Fan L. 2012. Biofouling of water treatment membranes: a review of the underlying causes, monitoring techniques and control measures. Membranes (Basel). 2:804–840. doi:10.3390/membranes2040804

Pinel ISM, Moed DH, Vrouwenvelder JS, van Loosdrecht MCM. 2020. Bacterial community dynamics and disinfection impact in cooling water systems. Water Res. 172:115505. doi:10.1016/j.watres.2020.115505

Prest EI, Hammes F, Kotzsch S, van Loosdrecht MCM, Vrouwenvelder JS. 2016. A systematic approach for the assessment of bacterial growth-controlling factors linked to biological stability of drinking water in distribution systems. Water Sci Technol Water Supply. 16:865–880. doi:10.2166/ws.2016.001

Rao TS, Kora AJ, Chandramohan P, Panigrahi BS, Narasimhan SV. 2009. Biofouling and microbial corrosion problem in the thermo-fluid heat exchanger and cooling water system of a nuclear test reactor. Biofouling. 25:581–591. doi:10.1080/08927010903016543

Roeselers G, Loosdrecht MCMv, Muyzer G. 2008. Phototrophic biofilms and their potential applications. J Appl Phycol. 20:227–235. doi:10.1007/s10811-007-9223-2

Roeselers G, Norris TB, Castenholz RW, Rysgaard S, Glud RN, Kühl M, Muyzer G. 2007. Diversity of phototrophic bacteria in microbial mats from Arctic hot springs (Greenland). Environ Microbiol. 9:26–38. doi:10.1111/j.1462-2920.2006.01103.x

Romano S, Schulz-Vogt HN, González JM, Bondarev V. 2015. Phosphate limitation induces drastic physiological changes, virulence-related gene expression, and secondary metabolite production in *Pseudovibrio* sp. Strain FO-BEG1. Appl Environ Microbiol. 81:3518–3528. doi:10.1128/AEM.04167-14

Rossi F, De Philippis R. 2015. Role of cyanobacterial exopolysaccharides in phototrophic biofilms and in complex microbial mats. Life (Basel). 5:1218–1238. doi:10.3390/life5021218

Russell JB, Cook GM. 1995. Energetics of bacterial growth: balance of anabolic and catabolic reactions. Microbiol Rev. 59:48–62. doi:10.1128/MMBR.59.1.48-62.1995

Samaddar S, Chatterjee P, Truu J, Anandham R, Kim S, Sa T. 2019. Long-term phosphorus limitation changes the bacterial community structure and functioning in paddy soils. Appl Soil Ecol. 134:111–115. doi:10.1016/j.apsoil.2018.10.016

Sanawar H, Pinel I, Farhat N, Bucs SS, Zlopasa J, Kruithof J, Witkamp G, van Loosdrecht M, Vrouwenvelder JS. 2018. Enhanced biofilm solubilization by urea in reverse osmosis membrane systems. Water Res X. 1:100004. doi:10.1016/j.wroa.2018.10.001

Sanawar H, Siddiqui A, Bucs SS, Farhat N, van Loosdrecht M, Kruithof J, Vrouwenvelder J. 2017. Applicability of short-term accelerated biofouling studies to predict long-term biofouling in reverse osmosis membrane systems. Desalin Water Treat. 97:72–78. doi:10.5004/dwt.2017.21625

Sandu C, Fulmer D, Nguyen K, Guo K, Felipe B. 2016. Non-phosphorus corrosion inhibitor optimizes cooling tower uptime for environmental compliance. Hydrocarb Process. Houston (TX): Gulf Publishing Co.

Seviour T, Derlon N, Dueholm MS, Flemming H-C, Girbal-Neuhauser E, Horn H, Kjelleberg S, van Loosdrecht MCM, Lotti T, Malpei MF, et al. 2019. Extracellular polymeric substances of biofilms: suffering from an identity crisis. Water Res. 151:1–7. doi:10.1016/j.watres.2018.11.020

Siddiqui A, Pinel I, Prest E, Bucs S, van Loosdrecht M, Kruithof J, Vrouwenvelder JS. 2017. Application of

DBNPA dosage for biofouling control in spiral wound membrane systems. Desalin Water Treat. 68:12–22. doi:10.5004/dwt.2017.20370

Smith EM, Prairie YT. 2004. Bacterial metabolism and growth efficiency in lakes: the importance of phosphorus availability. Limnol Oceanogr. 49:137–147. doi:10.4319/lo.2004.49.1.0137

Tchobanoglous G, Burton FL. 1991. Wastewater engineering treatment, disposal and reuse. New-York (NY): McGraw-Hill Inc.

Tsao H-F, Scheikl U, Herbold C, Indra A, Walochnik J, Horn M. 2019. The cooling tower water microbiota: seasonal dynamics and co-occurrence of bacterial and protist phylotypes. Water Res. 159:464–479. doi:10.1016/j.watres.2019.04.028

Türetgen I, Cotuk A. 2007. Monitoring of biofilm-associated *Legionella pneumophila* on different substrata in model cooling tower system. Environ Monit Assess. 125:271–279. doi:10.1007/s10661-006-9519-8

van der Kooij D, Hijnen WAM, Kruithof JC. 1989. The effects of ozonation, biological filtration and distribution on the concentration of easily assimilable organic carbon (AOC) in drinking water. Ozone-Sci Eng. 11:297–311. doi:10.1080/01919518908552443

Visvanathan C, Boonthanon N, Sathasivan A, Jegatheesan V. 2003. Pretreatment of seawater for biodegradable organic content removal using membrane bioreactor. Desalination. 153:133–140. doi:10.1016/S0011-9164(02)01114-1

Vrouwenvelder JS, Beyer F, Dahmani K, Hasan N, Galjaard G, Kruithof JC, Van Loosdrecht MCM. 2010. Phosphate limitation to control biofouling. Water Res. 44:3454–3466. doi:10.1016/j.watres.2010.03.026

Walker SL, Redman JA, Elimelech M. 2004. Role of cell surface lipopolysaccharides in *Escherichia coli* K12 adhesion and transport. Langmuir. 20:7736–7746. doi:10.1021/la049511f

Wang J, Liu M, Xiao H, Wu W, Xie M, Sun M, Zhu C, Li P. 2013. Bacterial community structure in cooling water and biofilm in an industrial recirculating cooling water system. Water Sci Technol. 68:940–947. doi:10.2166/wst.2013.334

Wang J, Wang D, Hou D. 2016. Hydroxyl carboxylate based non-phosphorus corrosion inhibition process for reclaimed water pipeline and downstream recirculating cooling water system. J Environ Sci (China). 39:13–21. doi:10.1016/j.jes.2015.10.007

Ward DM, Ferris MJ, Nold SC, Bateson MM. 1998. A natural view of microbial biodiversity within hot spring cyanobacterial mat communities. Microbiol Mol Biol Rev. 62:1353–1370.

Xu X, Stewart PS, Chen X. 2000. Transport limitation of chlorine disinfection of *Pseudomonas aeruginosa* entrapped in alginate beads. Biotechnol Bioeng. 49:93–100. doi:10.1002/(SICI)1097-0290(19960105)49:1<93::AID-BIT12>3.0.CO;2-C

Xue Z, Hessler CM, Panmanee W, Hassett DJ, Seo Y. 2013. *Pseudomonas aeruginosa* inactivation mechanism is affected by capsular extracellular polymeric substances reactivity with chlorine and monochloramine. FEMS Microbiol Ecol. 83:101–111. doi:10.1111/j.1574-6941.2012.01453.x

Zhu L, Qi H-Y, Lv M-L, Kong Y, Yu Y-W, Xu X-Y. 2012. Component analysis of extracellular polymeric substances (EPS) during aerobic sludge granulation using FTIR and 3D-EEM technologies. Bioresour Technol. 124:455–459. doi:10.1016/j.biortech.2012.08.059